



Degradation of Bisphenol S by heat activated persulfate: Kinetics study, transformation pathways and influences of co-existing chemicals

Qun Wang^{a,*}, Xiaohui Lu^{a,b}, Ye Cao^a, Jun Ma^b, Jin Jiang^b, Xiaofeng Bai^a, Tao Hu^a

^a Faculty of Geosciences and Environmental Engineering, Southwest Jiaotong University, Chengdu 610031, PR China

^b State Key Laboratory of Urban Water Resource and Environment, Harbin Institute of Technology, Harbin 150090, PR China

HIGHLIGHTS

- Parameters on the degradation of BPS by TAP technology were examined.
- Demisemi-lives method was used to determine the reaction orders.
- The relative contribution of SR and HR to BPS degradation were evaluated.
- Intermediates were identified, and possible degradation pathways were proposed.

ARTICLE INFO

Article history:

Received 1 April 2017

Received in revised form 24 June 2017

Accepted 7 July 2017

Available online 8 July 2017

Keywords:

Bisphenol S (BPS)

Thermo-activated persulfate oxidation

Kinetics study

Sulfate radical

Degradation pathways

ABSTRACT

Bisphenol S (BPS), which is an emerging estrogenic endocrine-disrupting chemical, was chosen as the model pollutant to study its degradation kinetics and mechanisms by thermo-activated persulfate (TAP) oxidation process in aqueous solution. A new method called demisemi-lives compared with the method of half-lives was proposed to investigate the kinetic parameters. In this new method, the $t_{1/4}$ were calculated via linear interpolation to analyze BPS decay. To ascertain the reaction order with regard to persulfate (PS) and BPS, a range of experiments were carried out, keeping the PS or BPS concentration constant, while changing the initial concentration of the other. The results revealed that the oxidation rate of BPS could be expressed by the kinetic rate equation $-d_{[BPS]}/dt = (2.39 \times 10^{-4} \text{ mM}^{-0.87} \text{ min}^{-1}) [BPS]^0 [PS]^{1.13}$ within the limiting experiment condition. Pseudo-zero-order mode and demisemi-lives method were applied to compute the pseudo-zero-order rate constant and obtain the value of the activation energy (E_a) of BPS reacted with PS subsequently by Arrhenius equation. The E_a is $112.9 \pm 6.8 \text{ kJ} \cdot \text{mol}^{-1}$, which is lower compared to its counterpart calculated from pseudo-first-order mode. The effects of initial pH, humic acid (HA), coexisting inorganic anions (i.e., carbonate/bicarbonate ($\text{CO}_3^{2-}/\text{HCO}_3^-$), nitrate ions (NO_3^-), chloride ions (Cl^-)) and radical scavenger (i.e., methyl alcohol (MeOH) and tertiary butanol (TBA)) on BPS degradation were evaluated. Ultra performance liquid chromatography-quadrupole-time of flight-mass spectrometry (LC-TOF-MS/MS) was employed to identify the intermediate products, and possible reaction pathways were proposed. To our best knowledge, this is the first study that reveals the kinetics and mechanisms of degradation of BPS in TAP system, and the proposed demisemi-lives method may be suitable for determining the kinetic order.

© 2017 Elsevier B.V. All rights reserved.

1. Introduction

Bisphenol A (BPA), considered as the representative of EDCs (endocrine disrupting chemicals), has been widely accepted as one of the most important monomers for the production of variety of chemical materials such as polycarbonate plastic resin and epoxy resin [1–4]. It has been reported that BPA exposure has related to the human diseases [5,6]. Therefore, relevant regulations

have been implemented to restrict its yield and applications [7]. For example, America, China and European Union banned the use of BPA based baby bottles in 2009, 2011 and 2011, respectively. Using substitution of BPA for manufacturers to observe these restrictions and regulations is consequently necessary [1]. Bisphenol-S (BPS; bis(4-hydroxyphenyl)sulfone), where two phenol ring are connected together by a sulfonyl group, is now widely used in various industrial applications due to its excellent thermostability and photostability and considered as a “safer” alternative to BPA [8,9]. For this reason, the production of BPS is increasing annually and is tend to exceed that of BPA [10]. It is

* Corresponding author.

E-mail address: xhlu_swjtu@126.com (Q. Wang).

noteworthy that BPS has been detected in lots of target object such as foodstuffs [11], paper products, currency bills [12], personal care products in both China and the US, and water bodies in China, Japan, Korea and India [13,14]. With the widespread presence of BPS in surroundings and a better dermal penetration than BPA, it is understandable that BPS has been found in the urine of the US and Asian population at concentrations ranging from 0.02 to 21.0 ng/mL [15]. However, the BPS shares the similar dilemma of acute toxicity, geno-toxicity, and estrogenic activity according to recent studies [16–18]. In addition, compared with BPA, BPS has been demonstrated to have a longer half-life but a reduced biodegradability [19]. Therefore, it is reasonable to eliminate the BPS from drinking water and wastewater just like BPA.

In recent years, advanced oxidation technologies have been proven highly effective to degrade organic compounds in water treatment by generation of highly powerful oxidants such as hydroxyl radicals ($\cdot\text{OH}$) (HR) and sulfate radicals ($\text{SO}_4\cdot^-$) (SR) which are able to destroy the structures of contaminants and transform them into small molecule compounds even water and carbon dioxide [20–23]. Among the various advanced oxidation processes (AOPs), sulfate radicals-based advanced oxidation processes (SR-AOPs) have gained great attention particularly in situ chemical oxidation (ISCO) [24]. The SR ($E_0 = 2.6\text{ V}$) can be generated by the activation of persulfate ($\text{S}_2\text{O}_8^{2-}$) and peroxymonosulfate (HSO_5^-) using various methods like heat [25,26], UV irradiation [27–29], transition metal [30–34], ultrasound (US) [35,36], base [37], activated-carbon [38], quinones and ozone [39,40].

Thermo-activated persulfate (TAP) is able to degrade many contaminants in aqueous systems, including benzene series [41], pesticides and pharmaceuticals [42–45]. Owing to without introduction of extra chemical, TAP is considered as a relatively clean method for the degradation of pollutants. Liang et al. investigated the oxidation of Trichloroethylene (TCE) and 1,1,1-Trichloroethane (TCA) by TAP in aqueous and soil slurry systems. The results revealed that TCE and TCA were difficult to degrade in soil systems compared with aqueous systems due to the presence of soil constituents, which could capture sulfate free radicals [46]. Huang et al. investigated treatability of 59 volatile organic compounds (VOCs) listed in the EPA SW-846 Method 8260B with TAP oxidation. The results showed that VOCs with carbon–carbon double bonds and benzene rings bonded to reactive functional groups can be rapidly degraded by persulfate oxidation, but halogenated alkanes were observed to have a relatively high resistance to the persulfate oxidation under the experimental conditions [47]. However, to the best of our knowledge, the degradation of BPS by TAP hasn't been reported.

In this work, the decomposition of BPS using TAP was investigated for the first time. Firstly, kinetic experiments were conducted to determine kinetics parameters of the BPS degradation at neutral pH and 60 °C by changing reactant concentration and keeping the concentration of the other constant. In these experiments, an improved method called demisemi-lives compared with the method of half-lives was proposed to explore the kinetic orders. Then, some important factors including temperature, solution pH, humic acid (HA), coexisting anions, were also evaluated. Finally, the intermediates products were analyzed by LC-TOF-MS/MS, and the reaction pathways of sulfate radical oxidation of BPS were proposed.

2. Materials and methods

2.1. Chemicals and reagents

Bisphenol-S (BPS, $\text{C}_{12}\text{H}_{10}\text{O}_4\text{S}$, 99.0%), potassium persulfate ($\text{K}_2\text{S}_2\text{O}_8$, 99.5%) were purchased from Sigma-Aldrich (Shanghai,

China). Methanol (HPLC, Thermo Fisher Scientific) and acetic acid were used for BPS determination. Tert-butyl-alcohol (t-butanol) was purchased from Tianjin Chemical Reagent Co., Ltd., China. All other chemicals were analytical grade without further purification and purchased from Sinopharm Chemical Reagent Company Ltd. (Shanghai, China). All the stock solutions were prepared by dissolving the chemical agents into Milli-Q water ($18.2\text{ M}\Omega\cdot\text{cm}$) prepared from a Millipore Milli-Q system and used within one week.

2.2. Experimental procedure

The stock aqueous of BPS (1 mM) and potassium persulfate (80 mM) were prepared before the experiments. All physiochemical characteristics of BPS are shown in Table 1. All the tests were conducted in 250 mL conical flasks containing 200 mL BPS solution. Flasks are immersed in the organic glass flume at predetermined temperature (55–70 °C) controlled by a thermostatic water bath (Tianheng Instrument Co., Ltd, Ningbo). The reactor was placed on a magnetic stirrer at 200 rpm. In the kinetics study of BPS degradation, adequate amounts of phosphate buffer (8 mM) was used to maintain constant solution pH and fixed ionic strength. Reaction was initiated by adding fixed dosage of PS. At given intervals of reaction, 1.4 mL of the solution was sampled in bottles, which contained 100 μL methanol as the quencher. Then, the sample was chilled in an ice bath to stop the reaction completely and analyzed within 24 h.

2.3. Analytical methods

The concentration of persulfate anions in the aqueous solution and mother liquor was analyzed by a spectrometric method using potassium iodide [48].

BPS was determined on a high-performance liquid chromatograph (HPLC) (Waters e2695) equipped with a Symmetry C18 column ($4.6\text{ mm} \times 150\text{ mm} \times 5\text{ }\mu\text{m}$, Waters) and a UV-visible detector (Waters 2998) at 258 nm. The eluent (1.000 mL/min) was a mixture of water (0.1% acetic acid) and methanol (V: V = 40:60). The injection volume was 100 μL and the column temperature was maintained at 35 °C. Total organic carbon (TOC) was measured using a TOC analyzer (multi N/C 3100, Germany). The pH of the aqueous solutions was measured by a combined glass electrode (E-201-C, Leici) connected to a PHS-3CW microprocessor pH/mVmeter (BANTE instrument). The byproducts of BPS were measured using ultra performance liquid chromatography-quadrupole-time of flight-mass spectrometry (SCIEX, X500R QTOF, USA). The negative mode electrospray ionization ((–) ESI) was conducted to analyze the mass spectra over a mass range of 50–500 m/z . The cone voltage used was 80.0 V conducted in auto full scan mode and a 10 μL volume was injected. The mobile phase comprised of acetonitrile (phase A) and 0.1% acetic acid (phase B) at a flow rate of 0.4 mL/min. The gradient increased to 95% B at 3 min in 7 min, and maintained from 10 min to 15 min, and then reverting to the initial condition (5% B) at 15 min in 1 min, and was then maintained until 20 min.

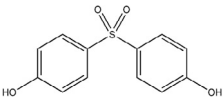
3. Results and discussion

3.1. Reaction kinetic orders

3.1.1. Kinetic model

It was assumed that BPS oxidation only followed sulfate radical pathways due to BPS is hardly degraded by direct reaction with PS (data not shown) and sulfate radical is the predominant radical at pH = 7. The overall degradation reaction of PS with BPS under

Table 1
Physiochemical characteristics of BPS.

Molecular structure	Molecular weight	Density (g/cm ³)	log K _{OW}	Melting point (°C)	Solubility (mg/L)
	250.27	1.366	1.65	240–241	909.0

constant temperature can be represented as the following equation:



According to Power Law model the global BPS degradation rate can be described by the following differential equation (Eq. (2)) [58]:

$$r = -d[\text{BPS}]/dt = k[\text{BPS}]^\alpha [\text{PS}]^\beta \quad (2)$$

where $r = -d[\text{BPS}]/dt$ is the rate equation for BPS degradation; k is the overall rate constant; α and β are the reaction orders with regard to BPS and PS, respectively. To ascertain the reaction orders of BPS and PS in the purpose of exploring a kinetics law of PS thermally oxidized BPS, the reaction will be carried out with excessive amounts of the oxidant (i.e., $[\text{PS}] \gg [\text{BPS}]$) to ensure the concentration of oxidant remains relatively constant. Therefore, Eq. (2) can be simply described as the follow equation: where $k_a = k[\text{PS}]^\beta$

$$r = d[\text{BPS}]/dt = k_a [\text{BPS}]^\alpha \quad (3)$$

3.1.2. Effect of BPS concentration under fixed PS concentration

In order to ascertain the reaction orders α , the first range of experiments were performed with a settled initial persulfate concentration (0.5 mM) and initial BPS concentrations altering from 0.00625 to 0.05 mM to ensure oxidant/contaminant molar ratios greater than 10/1. Phosphate buffer (i.e., $\text{HPO}_4^{2-}/\text{H}_2\text{PO}_4^-$) (8 mM) was applied to maintain constant solution pH (pH 6.8–7.0) and fixed ionic strength ($I \approx 0.016 \text{ M}$). The reaction rate constants of $\text{SO}_4^{\cdot-}/\text{HPO}_4^{2-}$ ($k = 1.2 \times 10^6 \text{ M}^{-1} \text{ s}^{-1}$) and $\text{SO}_4^{\cdot-}/\text{H}_2\text{PO}_4^-$ ($k = 7.0 \times 10^4 \text{ M}^{-1} \text{ s}^{-1}$) are slower compared to that of $\text{SO}_4^{\cdot-}$ with organic compounds ($\sim 10^9 \text{ M}^{-1} \text{ s}^{-1}$) [49]. Therefore, moderate concentration of phosphate-buffer may have no significant effect on the research of kinetics in thermally activated persulfate. In order to obtain a more precise kinetics study, it is reasonable to gather information of reaction at the very beginning. It is beneficial to reduce the influence of side reaction caused by intermediate products. For instance, the *method of initial rates* base on measuring the reaction rates in the very initial phase of reaction is commonly applied. The method requires suitable data points at the early stage of reaction to calculate the initial rate. Besides, the *method of half-lives* based on seeking the half-value period of a reaction according to the inlet concentration of one reactant when the other is maintain excess or

constant is also employed. Compared to initial rates method, the half-lives method could reveal more evincive reactant degradation behavior [50]. Ghauch et al. and Liang et al. used this method successfully for determining the reaction orders of ibuprofen (IBU) and trichloroethylene (TCE) degradation by TAP at 60 °C and 40 °C [50,51]. The results showed that the degradation of IBU and TCE was quarter and zero order with respect to organic reactant, respectively. However, the decay of reactant will reveal a tailing effect as the result of side reactions that would be evident when the reactant concentration is low. In present study, an improved method called demisemi-lives compared with the method of half-lives was proposed. The method is conducive to diminishing the influence of side reactions that can happen between the intermediate products and the SR, which may results in the extension of real full decay period, and thus obtain more accurate kinetic informations.

Rearranging and integrating Eq. (2) obtains:

$$\{[\text{BPS}]_t^{1-\alpha} - [\text{BPS}]_0^{1-\alpha}\} = k_a t (\alpha - 1) \quad (4)$$

The time for the BPS concentration to decay to three quarters of its initial value (i.e., $[\text{BPS}]_t = 3[\text{BPS}]_0/4$ and $t = t_{1/4}$) correlated with reaction order α can be described as follow:

$$t_{1/4} = \left\{ \left(\left(\frac{3}{4} \right)^{1-\alpha} - 1 \right) \cdot [\text{BPS}]_0^{1-\alpha} \right\} / [(\alpha - 1) \cdot k_a] \quad (5)$$

Assuming that $\alpha \neq 1$, the demisemi-life can be simplified as part of a function of initial BPS concentration to α and k_a (i.e., $F(\alpha, k_a)$) as follow:

$$t_{1/4} = F(\alpha, k_a) \cdot [\text{BPS}]_0^{1-\alpha} \quad (6)$$

Taking natural logarithms on both sides of Eq. (6) obtains:

$$\ln t_{1/4} = \ln F(\alpha, k_a) + (1 - \alpha) \ln [\text{BPS}]_0 \quad (7)$$

The demisemi-lives of BPS were calculated using the equations obtained via linear interpolation (see Table 2 and Fig. 1). Fig. 2 describes the relationship between $\ln(t_{1/4})$ and $\ln [\text{BPS}]_0$ conform to Eq. (7). The expression gives excellent linearity with a correlation coefficient $R^2 = 0.996$, and a slope of about 1.067 (± 0.041), which is equal to $(1 - \alpha)$. So, the reaction order with regard to BPS is -0.069 (i.e., $\alpha \approx 0$). The results showed that the reaction between PS and BPS is pseudo-zero -order for BPS. The conclusion

Table 2
Kinetic parameters for the determination of reaction orders for thermally activated persulfate oxidation of BPS at 60 °C with respect to BPS and Persulfate.

$[\text{BPS}]_0 \times 10^{-3} \text{ (mM)}$	$[\text{PS}]_0 \text{ (mM)}$	$[\text{PS}]_0/[\text{BPS}]_0$ molar ratio	Demisemi-life $t_{1/4}$ (min)	$K_a \times 10^{-4} \text{ (mM min}^{-1}\text{)}$
First Set of Experiments: Determination of Reaction Order α with Respect to BPS				
6.25	0.5 ± 0.02	80.0	14.1	1.11
12.5	0.5 ± 0.02	40.0	26.2	1.19
25.0	0.5 ± 0.02	20.0	60.2	1.04
50.0	0.5 ± 0.02	10.0	125.7	1.00
Second Set of Experiments: Determination of Reaction Order β with Respect to Persulfate				
25.0	0.25 ± 0.01	10.0	126.7	0.49
25.0	0.50 ± 0.02	20.0	55.1	1.13
25.0	1.0 ± 0.04	40.0	26.5	2.36
25.0	2.0 ± 0.08	80.0	12.4	5.04

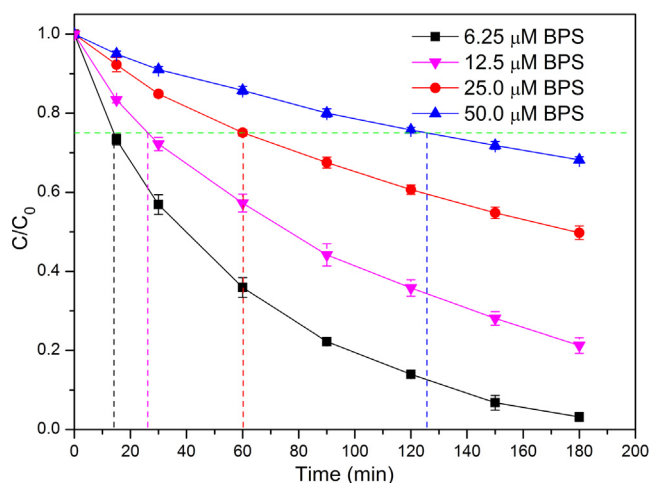


Fig. 1. Normalized measured BPS concentrations over time. Experimental conditions: $[I]_{PB} = 0.016$ M, $pH = 6.9 \pm 0.1$, temperature = 60 ± 1 °C, $[BPS]_0 = 6.25\text{--}50$ μ M, $[PS]_0 = 0.5$ mM.

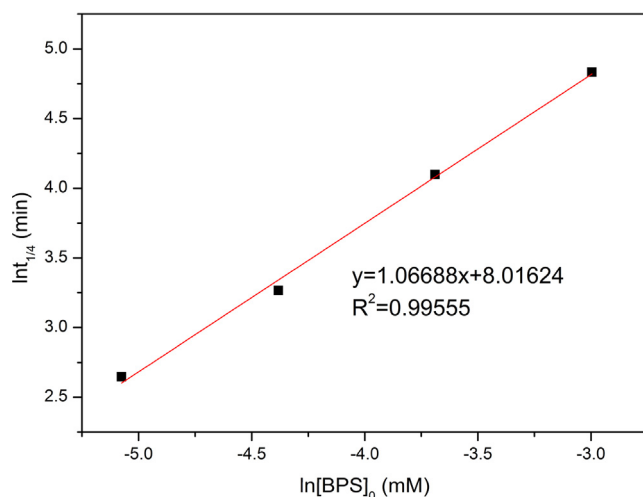


Fig. 2. Plot of $\ln(t_{1/2})$ vs. $\ln[BPS]_0$. A slope of $0.931 = 1 - \alpha$. Experimental conditions: $[I]_{PB} = 0.016$ M, $pH = 6.9 \pm 0.1$, temperature = 60 ± 1 °C, $[BPS]_0 = 6.25\text{--}50$ μ M, $[PS]_0 = 0.5$ mM.

was identical to one reported by Liang et al. [50] but different from Ghauch et al. [51], who found a quarter order reaction ($\alpha = 0.24$) with respect to IBU. The authors considered that the discrepancy was mainly due to the high density of phosphate, which might result in considerable scavenging rate of SR. Generally, the generation rate of SR is constant under a fixed temperature and an unaltered initial persulfate concentration. As constant reaction rate between sulfate radical and organics is usually very high, the sulfate radical is consumed rapidly once they are produced, which results in very low steady state concentration of sulfate radical. Therefore, the amount of organic molecules degraded by sulfate radical per unit time is almost constant under the same condition (i.e., with the same temperature and initial persulfate concentration). That is, the destruction rate of organics is independent of the initial organics concentration (i.e., zero order reaction with respect to organics) and determined by the generation rate of SR.

On the other hand, in the study reported by Ghauch et al., just as the analysis of authors, the effects of high phosphate concentration could not be neglected. In the competitive reaction, increasing IBU

concentration can capture more SR which results in acceleration of IBU oxidation and observing nonzero order with respect to IBU.

As for BPS degradation, it follows a pseudo-zero-order reaction and an average rate constant of $(1.09 \pm 0.1) \times 10^{-4}$ mM min^{-1} calculated by the equation (Eq. (8)) which derived from the zero-order reaction rate equation.

$$k_x = [BPS]_0 / 4t_{1/4} \quad (8)$$

3.1.3. Effect of PS concentration under fixed BPS concentration

In the next experiments, varying initial persulfate concentrations (i.e., 0.25–2.0 mM) were carried out while keeping the identical initial BPS concentration (i.e., 0.025 mM). The purpose of those experiments was to investigate the reaction order β in PS. The following equation can be obtained by transforming and rearranging Eqs. (2) and (3).

$$k_x = k \cdot [PS]_t^\beta \approx k \cdot [PS]_{t=0}^\beta \quad (9)$$

Taking natural logarithms on both sides of Eq. (9) leads to:

$$\ln k_x = \ln k + \beta \ln [PS]_t \approx \ln k + \beta \ln [PS]_{t=0} \quad (10)$$

The experimental data with normalized $[BPS]_t/[BPS]_0$ were shown in Fig. 3. The resulting PS/BPS molar ratios changed from 10.0 to 80.0 and the $t_{1/4}$ were also calculated using linear interpolation. The computed k_a values using Eq. (8) are also shown in Table 2. The linearity of the $\ln(k_a)$ and $\ln[PS]_0$ was excellent with the correlation coefficient equal to 0.999 (Fig. 4). Consequently, the straight slope obtained (slope = 1.10) equivalent to the reaction order β with regard to PS according to Eq. (10). The reaction orders with respect to BPS and PS were 0 and 1.1 obtained in the present study, respectively.

Based on previous analysis, the degradation rate of BPS depends on the formation rate of sulfate radical. Under the same temperature, the generation rate of sulfate radical is directly proportional to the PS dosage. Therefore, first-order reaction with respect to PS should be observed in the experiment. This discrepancy perhaps caused by the decay of PS as the reaction progresses, which would be evident with the decrease in the initial PS concentration. Consequently, subnormal k_a were calculated due to the extended $t_{1/4}$ in low dosage of PS and non-first order reaction was obtained.

Then, the overall rate constant of the reaction (k) can be gained from the intercept shown in Fig. 4 according to Eq. (10). The

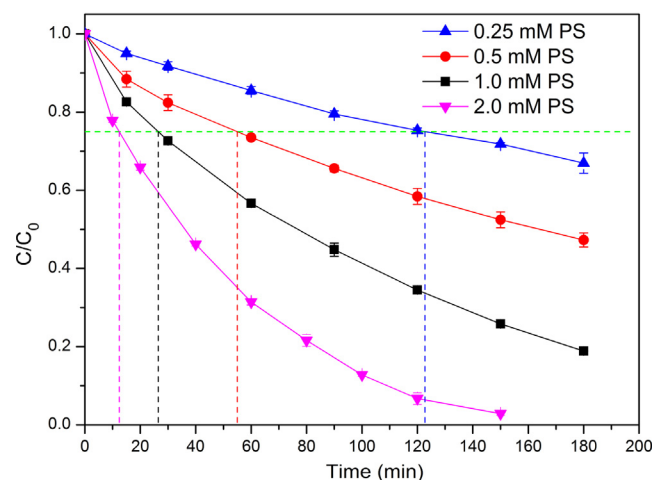


Fig. 3. Normalized measured BPS concentrations over time. Experimental conditions: $[I]_{PB} = 0.016$ M, $pH = 6.9 \pm 0.1$, temperature = 60 ± 1 °C, $[BPS]_0 = 25$ μ M, $[PS]_0 = 0.25\text{--}2.0$ mM.

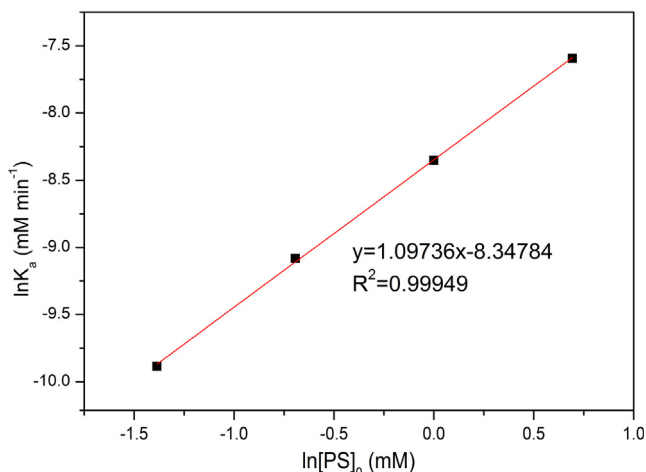


Fig. 4. Plot of $\ln(k_a)$ vs. $\ln[PS]$. A slope of $1.13 = \beta$. Experimental conditions: $[I]_{PB} = 0.016$ M, $pH = 6.9 \pm 0.1$, temperature = 60 ± 1 °C, $[BPS]_0 = 25$ μ M, $[PS]_0 = 0.25$ – 2.0 mM.

intercept value was -8.35 and the average overall rate constant was calculated to be $2.36 \times 10^{-4} \text{ mM}^{1-(\alpha+\beta)} \text{ min}^{-1}$. So, the reaction law between PS and BPS would be expressed as the following equation (Eq. (11)):

$$r = -d[BPS]/dt = k[BPS]^\alpha [PS]^\beta$$

$$= (2.36 \times 10^{-4} \text{ mM}^{1-(\alpha+\beta)} \text{ min}^{-1}) \times [BPS]^{\alpha=0} [PS]^{\beta=1.1} \quad (11)$$

This law is applicable to describe the BPS degradation rate under given conditions in this literature (i.e., a constant ionic strength of 0.016 , a temperature of 60 °C, and pH 7).

As mentioned above, obtaining reaction information in the initial reaction period is important for determining the order of reaction. The method of demisemi-lives may be unsuitable or inaccuracy when the lower temperature is applied or organic contaminants concentration is high (i.e., the demisemi-lives are prolonged). For example, all the above experimental are conducted at 50 °C and different orders with regard to BPS and PS are observed (data not shown). In fact, equation 4–8 can be generalize and get a common approach (see SI, Text. 2S). The orders of reac-

tion are exactly consistent with what we have determined before when decimus-lives method is applied (see SI, Fig. 3S and Fig. 4S).

3.2. Effect of temperature

Temperature plays an especially important role in thermo-activated PS oxidation. Increasing temperature results in accelerating decomposition of PS, thus increasing the production of SR and promoting the degradation of BPS. On the basis of the kinetics study, the oxidation of BPS can be expressed by pseudo-zero-order kinetics model described by the following equations (Eqs. (12) and (13)).

$$\frac{d[BPS]}{dt} = -k \quad (12)$$

$$\frac{[BPS]_t}{[BPS]_0} = 1 - \frac{k}{[BPS]_0} t \quad (13)$$

where k represents the zero order rate constant, $[BPS]_0$ and $[BPS]_t$ are the molar concentrations of BPS before reaction and in the reaction process. The k was obtained by the equation: $k = [BPS]_0/(4t_{1/4})$. The $t_{1/4}$ represents the time for a quarter of the initial BPS content to be destroyed by SR and is calculated via linear interpolation. Fig. 5a reveals the normalized BPS concentrations $[BPS]_t/[BPS]_0$ decay over time at different temperature (55 – 70 °C). No BPS decomposition is observed for reactions carried out at 70 °C without PS in 3 h, indicating it's good thermostability and the disappearance of BPS was mainly due to the active species (i.e., SR or HR) generated in the TAP system. When the temperature was 55 °C, the removal rate of BPS was 48.4% over 180 min in TAP system; almost a complete BPS removal was achieved within 120 min while the temperature was elevated to 70 °C. The BPS degradation rate constants continuously increased from $1.29 \times 10^{-6} \text{ mol} \cdot \text{m}^{-3} \cdot \text{s}^{-1}$ to $8.11 \times 10^{-6} \text{ mol} \cdot \text{m}^{-3} \cdot \text{s}^{-1}$ when the temperature was raised from 55 °C to 70 °C. Accordingly, demisemi-life time of BPS was dwindled from 80.9 to 12.8 min.

As shown in the Fig. 5b, $\ln k$ decreased linearly with $1/T$, and this relationship fits the Arrhenius equation well ($R^2 = 0.989$) (Eq. (14)).

$$\ln k = \ln A - E_a/RT \quad (14)$$

where A is the pre-exponential factor (unit of k), E_a is the activation energy, R is the universal gas constant ($8.314 \text{ J mol}^{-1} \text{ K}^{-1}$), and T is the absolute temperature. The E_a was calculated to be (112.9 ± 6.8)

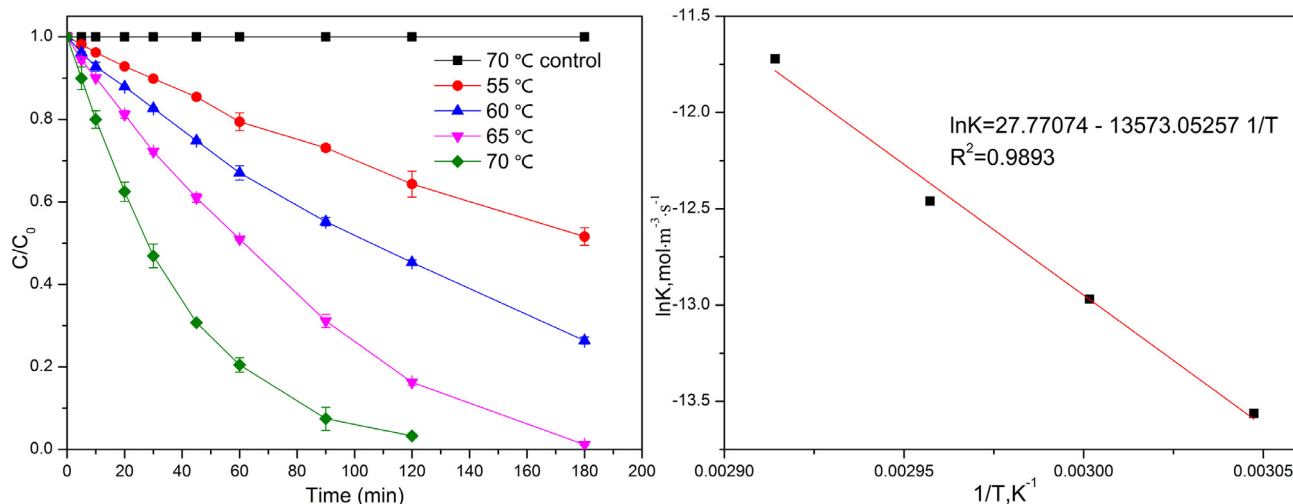


Fig. 5. (a) Pseudo-zero-order degradation of BPS at different temperatures; (b) plot of $\ln k$ vs $1/T$ for E_a estimation via Arrhenius equation. Experimental conditions: $[BPS]_0 = 25$ μ M; $[PS]_0 = 0.5$ mM; $[pH]_0 = 5.5$; $T = 55$ – 70 °C; reaction time = 180 min.

$\text{kJ}\cdot\text{mol}^{-1}$ according to the linear slope revealed in Fig. 5b. This E_a value was close to those obtained for p-nitrophenol ($127.8 \pm 1.56 \text{ kJ}\cdot\text{mol}^{-1}$) [41], sulfamethazine ($126 \text{ kJ}\cdot\text{mol}^{-1}$) [52], atrazine ($141 \text{ kJ}\cdot\text{mol}^{-1}$) [43], and bisoprolol ($119.8 \pm 10.8 \text{ kJ}\cdot\text{mol}^{-1}$) [45] oxidation by thermo-activated persulfate.

It is noteworthy that the decomposing rate of BPS decreases over time gradually, which follows pseudo-first-order behavior that tends to be more evident when the temperature is high. The most likely explanation for this behavior was the generation of by products instead of the variation of its own concentration (i.e., rule of first order reaction), although the data were fitted using the pseudo-first-order model also exhibited good correlations ($0.976 < R^2 < 0.998$) (Fig. 1S, Supplementary material). Moreover, the activation energy calculated from pseudo-first-order mode ($126.9 \pm 1.8 \text{ kJ}\cdot\text{mol}^{-1}$) was higher than that from pseudo-zero-order mode (Fig. 1S, Supplementary material). Generally, if the degradation of pollutants follows pseudo-zero-order kinetics model, the activation energy calculated from pseudo-first-order mode will have a higher value compared with that from pseudo-zero-order mode (see SI, Fig. 2S and Text. 1S). Therefore, the kinetic orders of contaminants in heat activated persulfate system cannot be neglected when the activation energy of the reaction of contaminants with PS needs to be calculated.

3.3. Effect of coexisting inorganic anions and HA

The effect of inorganic anions and HA has been investigated through adding different concentrations of inorganic anions and

HA vary from 5 mM to 50 mM and from 0.5 mgC/L to 5.0 mgC/L, respectively. Fig. 6 reveals the graph of $[\text{BPS}]/[\text{BPS}]_0$ under different inorganic anion and HA vary from time. As shown, different inorganic anions exhibit different inhibiting effects on the BPS degradation. No addition of inorganic anions and HA, the degradation rate of BPS was 75.6% (data not shown). In the presence of 5 mM HCO_3^- , Cl^- , NO_3^- and 0.5 mgC/L HA, the degrading efficiency of BPS was 54.0%, 78.0%, 74.5%, and 60.3%, respectively. However, when the concentration of inorganic anions and HA increased to 50 mM and 5 mgC/L, the degradation rate of BPS decreased to 52.7%, 62.0%, 71.4%, and 34.0%, respectively.

NO_3^- could only slightly influence BPS degradation because it almost did not react with SR ($5.0 \times 10^4 \text{ M}^{-1} \text{ s}^{-1}$). The dual role of Cl^- in BPS degradation was observed. At low concentration ($[\text{Cl}^-] = 5 \text{ mM}$), the BPS removal rate increased slightly, whereas the value decreased when the concentration of Cl^- ($[\text{Cl}^-] > 5 \text{ mM}$) increased. Previous studies also observed that the effects of chloride on the degradation of contaminants was concentration-dependent [53]. Cl^- can react with SR to generate relatively weaker species Cl^\cdot ($E_0(\text{Cl}^\cdot/\text{Cl}^-) = 2.4 \text{ V}$) (Eq. (21)). When the level of chloride is low, Cl^\cdot may degrade BPS and reduce the recombination of SR thus promote the destruction of BPS slightly. However, the removal rate of BPS reduced with increasing Cl^- concentration, which may due to the scavenging of $\text{SO}_4^{\cdot-}$ and generation of less reactive chlorine species such as Cl_2^- and HOCl (Eqs. (15)–(21)) [54].

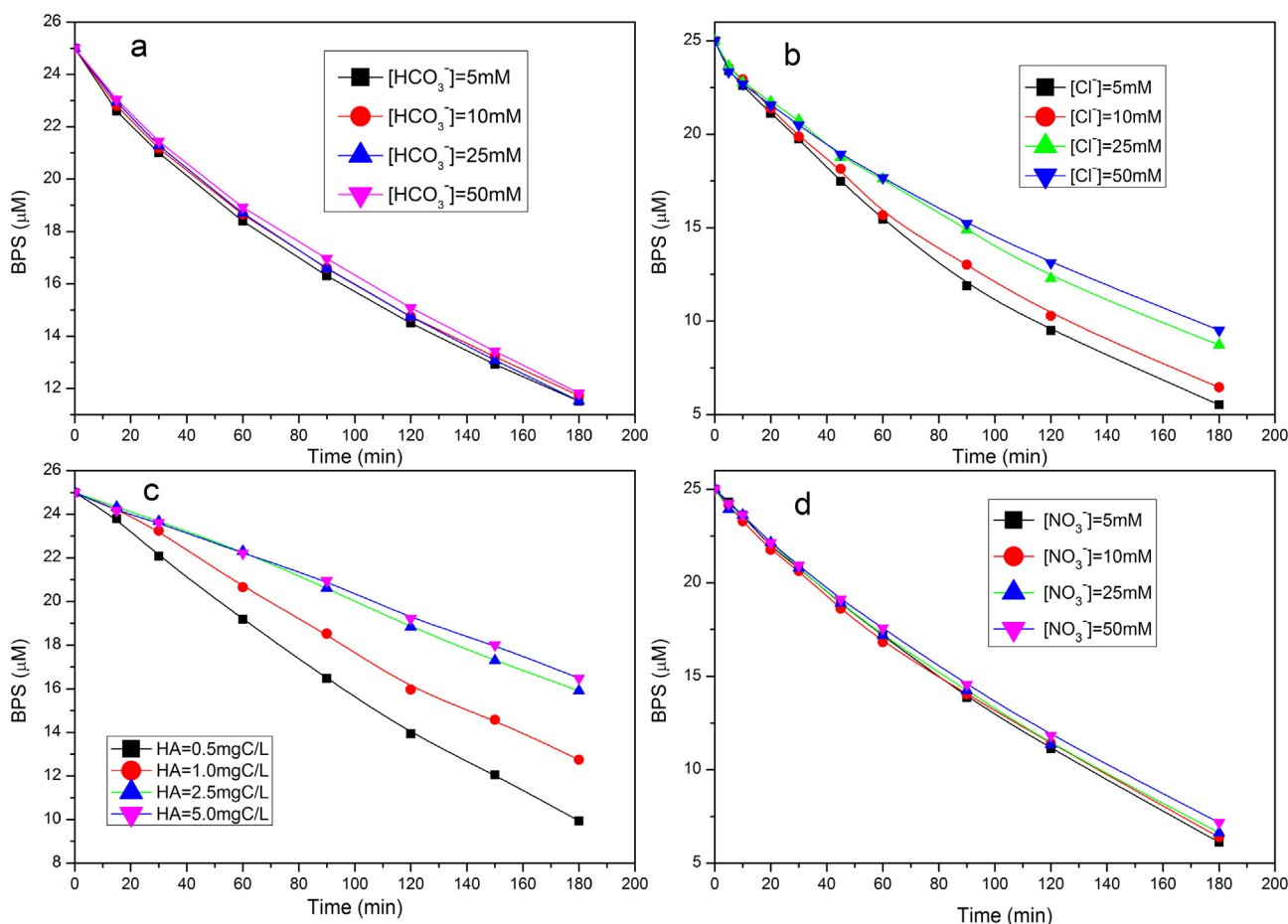
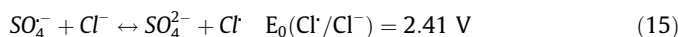


Fig. 6. Effects of (a) bicarbonate, (b) chloride, (c) HA, and (d) nitrate on BPS oxidation by heat-activated persulfate. Experimental conditions: temperature = $60 \pm 1^\circ\text{C}$, $[\text{BPS}]_0 = 25 \mu\text{M}$, $[\text{PS}]_0 = 0.5 \text{ mM}$, unbuffered, reaction time = 180 min.

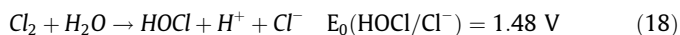
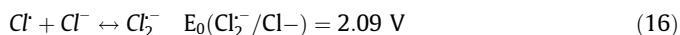
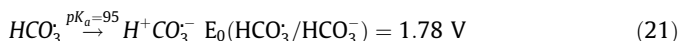
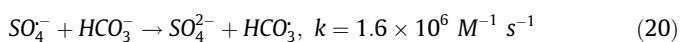
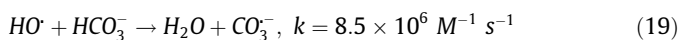


Fig. 6a depicts the impact of the carbonate/bicarbonate ($[\text{HCO}_3^-]_0/[\text{PS}]_0 = 10:1$ to $100:1$) on the decay of BPS. Bicarbonate is the good scavengers for HR and SR, as the following equations [54]:



pH changes (8.6 ± 0.15) was not obvious in the reaction due to the buffer function of bicarbonate. On the surface, the introduction of bicarbonate significantly inhibited the removal rate of BPS. The inhibition only showed slight increases, while increasing the concentration of bicarbonate. Perhaps HCO_3^- could degrade BPS effectively and the inhibition was mainly caused by the basic environment (3.4). The presence of HA significantly influences the degradation of BPS, removal rate of BPS decreased with additional HA observably (Fig. 6c). HA that contains carboxyl and hydroxyl functional groups could compete with BPS for HR and SR in solution, which results in consumption of oxidants and diminution of removal rate.

3.4. Effect of pH and study of predominant radical species

Solution pH is one of the most important factors in chemical reaction. No buffer was used in this experiment owing to the influence of phosphate in TAP system. The effect of pH (3.0–11.0) on the BPS degradation in this study was shown in Fig. 7. Complete removal rate was observed at pH 3.0, followed by pH 6.0 (91%), pH 8.0 (78%) and pH 11.0 (61%). Minghua Nie et al. used TAP system to decompose chloramphenicol, showing the removal rate of pollutant decreased as the solution pH increased from 3.06 to 10.97 [53]. It was reported that more SR could be generated through acid-catalyzation in acidic environment [55], which might facilitate the BPS degradation. And this catalysis decreases with pH increase thus hinder the decomposition of BPS. At alkaline environment, it is well known that SR rapidly consumed by hydroxyl ions and converted to HR. Although the hydroxyl radical possesses higher redox potential compared with sulfate radical, the suppressed degradation of BPS was observed, perhaps because hydroxyl radical decay more rapidly by nontarget species. That is, the utilization level of persulfate is reduced at basic pH.

To understand which radical species mainly responsible for the degradation of BPS at varying pH, experiments with the addition of radical scavengers were conducted. Methanol (MeOH) with α -H reacts with $\cdot\text{OH}$ at a rate dozens of times greater than that with $\text{SO}_4^{\cdot-}$ ($k_{\text{MeOH}/\cdot\text{OH}} = (1.2 - 2.8) \times 10^9 \text{ M}^{-1} \text{ s}^{-1}$, $k_{\text{MeOH}/\text{SO}_4^{\cdot-}} = (1.6 - 7.7) \times 10^7 \text{ M}^{-1} \text{ s}^{-1}$). Unlike MeOH, the reaction rate of Tert-butanol (TBA) without α -H reacts with $\text{SO}_4^{\cdot-}$ was much slower than

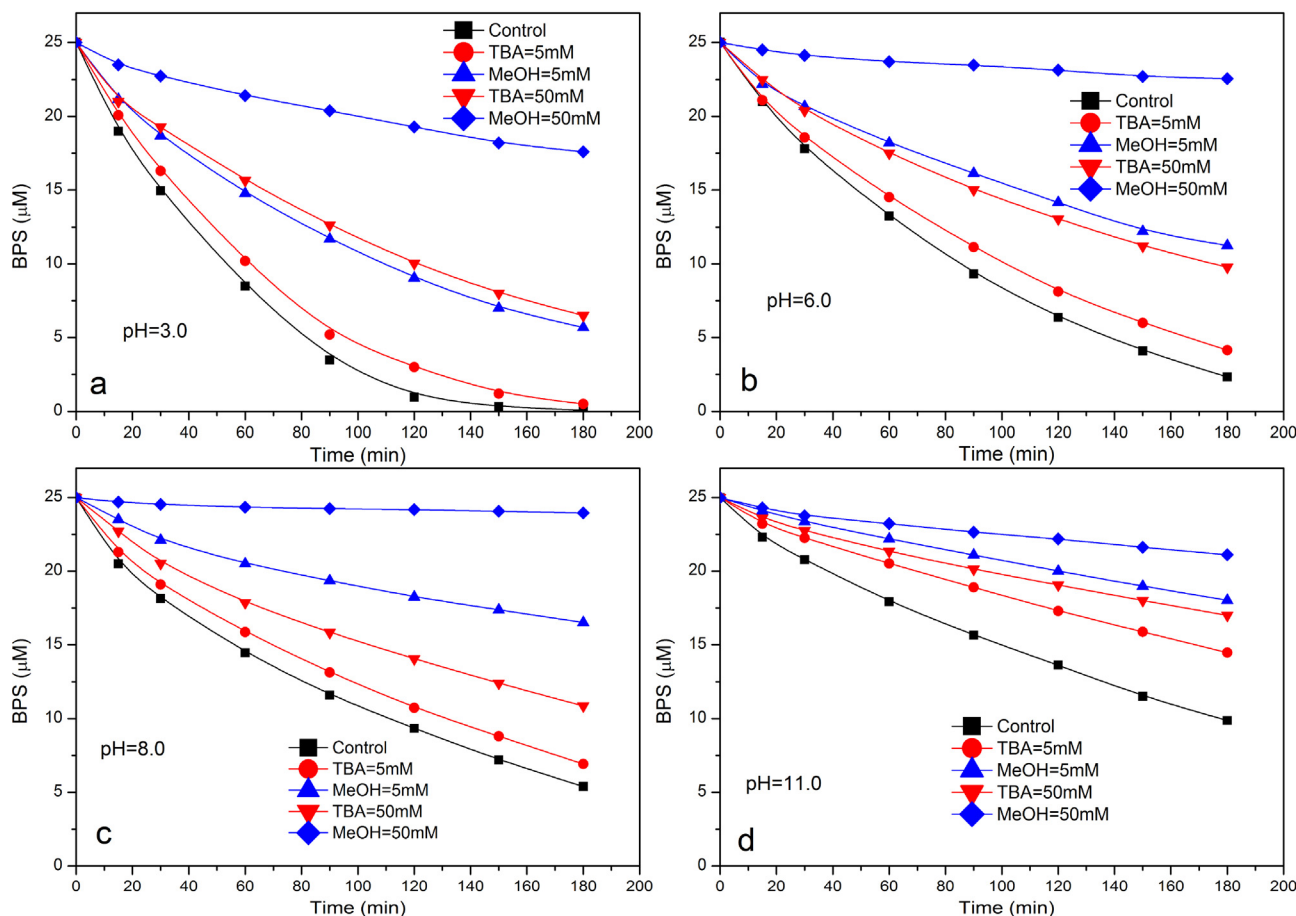


Fig. 7. Effects of MeOH and TBA as radical scavenger on BPS oxidation by heat-activated persulfate: (a) pH 3.0, (b) pH 6.0, (c) pH 8.0, and (d) 11.0. Experimental conditions: $[\text{BPS}]_0 = 25 \mu\text{M}$, $[\text{PS}]_0 = 0.5 \text{ mM}$, $T = 60 \pm 1^\circ\text{C}$, unbuffered, reaction time = 180 min.

Table 3
Radical identification parameters at different pH.

Additive	pH	k_{obs} (10^{-2} min^{-1})	R^2	% change in k_{obs}
No addition of alcohol	3.0	2.40 ± 0.18	0.972	
	6.0	1.23 ± 0.05	0.992	
	8.0	0.85 ± 0.02	0.998	
	11.0	0.52 ± 0.01	0.999	
TBA	3.0	1.98 ± 0.08	0.988	–17.5
	6.0	0.96 ± 0.01	0.998	–22.0
	8.0	0.71 ± 0.01	0.998	–16.5
	11.0	0.31 ± 0.004	0.999	–40.4
MeOH	3.0	0.84 ± 0.01	0.999	–65.0
	6.0	0.47 ± 0.01	0.995	–61.8
	8.0	0.25 ± 0.01	0.983	–70.6
	11.0	0.19 ± 0.003	0.999	–63.5

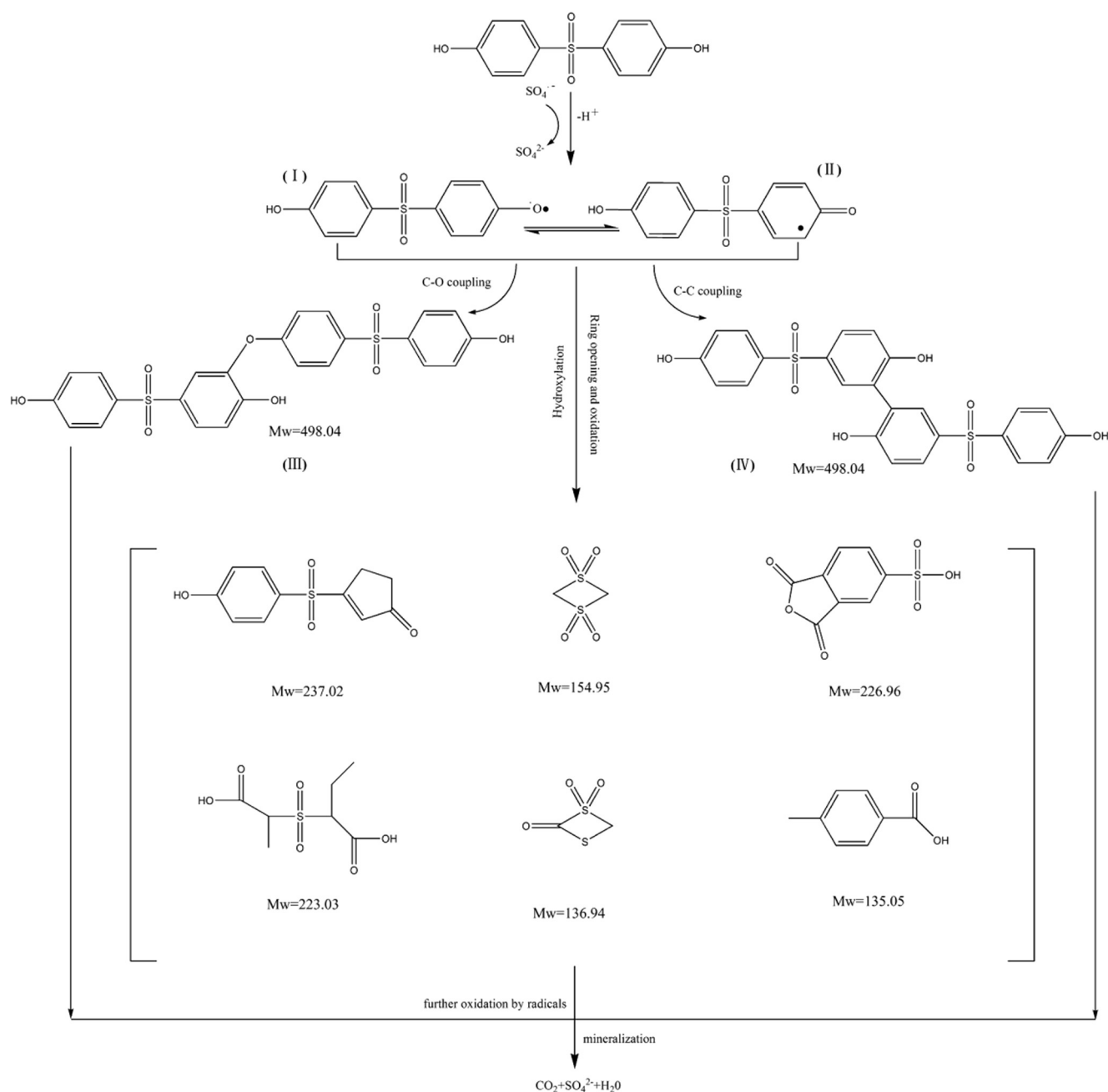


Fig. 8. Proposed possible transformation pathways for BPS degradation in thermo-activated PS oxidation process.

that with $\cdot\text{OH}$ ($k_{\text{TBA}/\cdot\text{OH}} = (3.8 - 7.6) \times 10^8 \text{ M}^{-1} \text{ s}^{-1}$, $k_{\text{TBA}/\text{SO}_4^{\cdot-}} = (4.0 - 9.1) \times 10^5 \text{ M}^{-1} \text{ s}^{-1}$) [38]. Fig. 7 and Table 3 present the effect of different radical scavenger dosages (5 mM and 50 mM) on the degradation of BPS. As shown, a significant decrease in the oxidation rate of BPS in the presence of alcohols at any specific pH. Obviously, the inhibition of TBA on BPS degradation was less than that of MeOH over the tested pH range (3.0–11.0). In Table 3, the k_{obs} obtained from different pHs (3.0–11.0) in the presence of 5 mM alcohols. As it can be noticed, in the presence of TBA, the % change in k_{obs} ($(k_{\text{obs}}(\text{with alcohol})/k_{\text{obs}}(\text{alcohol free at same pH}) - 1) \times 100$) values were close (–17.5, –22.0 and –16.5) at pH 3.0, 6.0 and 8.0. However, when the pH was increased to 11.0, the % change in k_{obs} observably dropped to –40.4. The % change in k_{obs} showed little change while in the presence of MeOH at tested pH (3.0–11.0). These findings corroborate that $\text{SO}_4^{\cdot-}$ was the most likely dominant radical species at pH 3.0–9.0, and the relative contribution of HR to the degradation gradually increased at a basic condition (see SI, Text. 3S and Fig. 5S). Furthermore, the generation of HR at alkaline condition was further verified by EPR experiments (see SI, Fig. 6S). These results are consistent with previous reports [43,56].

3.5. Reaction pathway of BPS degradation

In the ultraviolet region, BPS absorption spectrum has two absorption peaks located at 233 nm and 258 nm, respectively. Fig. S7 describes the UV–vis spectra of the samples drawn at different time at 60 °C, and PS/BPS molar ratio 40/1. The peak height of two absorption peaks decreased over reaction time, indicating the destruction of BPS. But the absorbance from 210 nm to 230 nm was increased with BPS degradation, which may be due to the generation of degradation products.

A total of twelve intermediate products were detected and identified partially by LC–TOF–MS/MS (see SI, Table S1). By the analysis of mass spectra, the identified degradation products were shown in Fig. 8. Referred to these compounds, two possible transformation pathways have been proposed. Generally, the SR reacts with substrate via direct electron transfer reaction [57]. In the proposed pathways, oxidation of BPS is initiated by abstracting an electron to the oxide, forming BPS radicals (I and II). On the one hand, these radicals react with each other and thereafter produce resultant dimers (III and IV) by carbon-carbon (C–C) and carbon-oxygen (C–O) coupling. Many of the products contain more than two sulfur atoms (see SI, Table S1), perhaps because the coupling reactions between BPS radicals and sulfate radical were also proceeded. On the other hand, these BPS radicals could be oxidized to a series of intermediate products by transferring electron unceasingly. Finally, these intermediate products were mineralized to CO_2 , H_2O and SO_4^{2-} by further oxidation.

Fig. S8 depicts the TOC values as a function of treatment time. The initial TOC is $3.58 \pm 0.07 \text{ mg/L}$, which accord with the TOC of 25 μM BPS (i.e. 3.60 mg/L). The TOC removal was 27.0% after 180 min at 60 °C, almost complete TOC removal was observed after 180 min when the temperature increased to 70 °C. The TOC values decrease with the degradation of BPS, and the TOC removal rate was accelerated when the BPS was degraded almost completely. Fig. S9 summarizes the residual concentration of PS and the values of the $\Delta[\text{BPS}]/\Delta[\text{PS}]$ in TAP system at 60 °C and 70 °C, respectively. As it can be noticed, the decomposition rate of PS increased significantly when the temperature raised from 60 °C to 70 °C, but the values of the $\Delta[\text{BPS}]/\Delta[\text{PS}]$ of 70 °C were generally lower than that of 60 °C. This may due to the hydrolysis of PS at 70 °C more strong compared with PS hydrolysis at 60 °C, which result in a lower pH (see SI, Fig. S9b). As for BPS abatement, not only is excessively high temperature energy-intensive but also PS is more low-efficiency, though BPS is degraded much faster. Both effectiveness and

economy should be taken into consideration when TAP system is applied to the degradation of BPS.

4. Conclusions

In the present work, TAP can effectively oxidize BPS. The kinetic reaction order, varying influence factors and possible transformation pathways were explored. The following conclusions could be summarized from this work:

- (i). The BPS and its TOC removal rate increased significantly with increasing temperature. The activation energy of the BPS treatment was determined as $112.9 \pm 6.8 \text{ kJ} \cdot \text{mol}^{-1}$.
- (ii). The degradation rate of BPS by potassium persulfate could be described by the kinetic rate equation: $-\text{d}[\text{BPS}]/\text{dt} = (2.39 \times 10^{-4} \text{ mM}^{-0.1} \text{ min}^{-1})[\text{BPS}]^0[\text{PS}]^{1.1}$ with the limits of the experimental conditions used here. And the proposed demisemi-lives method may be suitable for determining kinetic order.
- (iii). The effects of the presence of the NO_3^- anions on BPS degradation were negligible. The Cl^- anions has dual role on BPS oxidation. By contrast, HCO_3^- , and HA could significantly slow down the degradation rate of BPS. $\text{SO}_4^{\cdot-}$ contributed substantially to BPS degradation under an acidic and neutral condition, in particular, the relative contribution of HR to the degradation gradually increased at a basic condition. The decomposition of PS could be accelerated under low pH, and thus the degradation rate of BPS increased with the pH reducing.
- (iv). Generation of BPS radicals was the startup process of BPS degradation and the formation of dimers was one of the BPS degradation pathways.

Acknowledgments

This research was financially supported by the National Natural Science Foundation of China (No. 51378141). We also thank Dr. Congwei Luo, Dr. Peng Zhou and Dr. Da Wang for fruitful discussion.

Appendix A. Supplementary data

Supplementary data associated with this article can be found, in the online version, at <http://dx.doi.org/10.1016/j.cej.2017.07.041>.

References

- [1] R. Kuruto-Niwa, Y. Terao, R. Nozawa, Identification of estrogenic activity of chlorinated bisphenol A using a GFP expression system, *Environ. Toxicol. Pharmacol.* 12 (2002) 27–35.
- [2] G.V. Korshin, J. Kim, L. Gan, Comparative study of reactions of endocrine disruptors bisphenol A and diethylstilbestrol in electrochemical treatment and chlorination, *Water Res.* 40 (2006) 1070–1078.
- [3] P.E. Stackelberg, E.T. Furlong, M.T. Meyer, S.D. Zaugg, A.K. Henderson, D.B. Reissman, Persistence of pharmaceutical compounds and other organic wastewater contaminants in a conventional drinking-water-treatment plant, *Sci. Total Environ.* 329 (2004) 99–113.
- [4] A. Usman, M. Ahmad, From BPA to its analogues: is it a safe journey?, *Chemosphere* 158 (2016) 131–142.
- [5] Y.Q. Huang, C.K. Wong, J.S. Zheng, H. Bouwman, R. Barra, B. Wahlstrom, L. Neretin, M.H. Wong, Bisphenol A (BPA) in China: a review of sources, environmental levels, and potential human health impacts, *Environ. Int.* 42 (2012) 91–99.
- [6] M.J. Roelofs, M. van den Berg, T.F. Bovee, A.H. Piersma, M.B. van Duursen, Structural bisphenol analogues differentially target steroidogenesis in murine MA-10 Leydig cells as well as the glucocorticoid receptor, *Toxicology* 329 (2015) 10–20.
- [7] E. Yamazaki, N. Yamashita, S. Taniyasu, J. Lam, P.K. Lam, H.B. Moon, Y. Jeong, P. Kannan, H. Achyuthan, N. Munuswamy, K. Kannan, Bisphenol A and other

- bisphenol analogues including BPS and BPF in surface water samples from Japan, China, Korea and India, *Ecotoxicol. Environ. Saf.* 122 (2015) 565–572.
- [8] R. Kuruto-Niwa, R. Nozawa, T. Miyakoshi, T. Shiozawa, Y. Terao, Estrogenic activity of alkylphenols, bisphenol S, and their chlorinated derivatives using a GFP expression system, *Environ. Toxicol. Pharmacol.* 19 (2005) 121–130.
 - [9] M.Y. Chen, M. Ike, M. Fujita, Acute toxicity, mutagenicity, and estrogenicity of bisphenol-A and other bisphenols, *Environ. Toxicol.* 17 (2002) 80–86.
 - [10] J.M. Molina-Molina, E. Amaya, M. Grimaldi, J.M. Saenz, M. Real, M.F. Fernandez, P. Balaguer, N. Olea, In vitro study on the agonistic and antagonistic activities of bisphenol-S and other bisphenol-A congeners and derivatives via nuclear receptors, *Toxicol. Appl. Pharmacol.* 272 (2013) 127–136.
 - [11] C. Liao, K. Kannan, A survey of bisphenol A and other bisphenol analogues in foodstuffs from nine cities in China, *Food Addit. Contam. Part A, Chemistry, Analysis, Control, Exposure & Risk Assessment* 31 (2014) 319–329.
 - [12] C. Liao, F. Liu, K. Kannan, Bisphenol S, a new bisphenol analogue, in paper products and currency bills and its association with bisphenol A residues, *Environ. Sci. Technol.* 46 (2012) 6515–6522.
 - [13] H. Guo, H. Li, N. Liang, F. Chen, S. Liao, D. Zhang, M. Wu, B. Pan, Structural benefits of bisphenol S and its analogs resulting in their high sorption on carbon nanotubes and graphite, *Environ. Sci. Pollut. Res.* 23 (2016) 8976–8984.
 - [14] H. Jin, L. Zhu, Occurrence and partitioning of bisphenol analogues in water and sediment from Liaoh River Basin and Taihu Lake China, *Water Res.* 103 (2016) 343–351.
 - [15] C. Liao, F. Liu, H. Alomirah, V.D. Loi, M.A. Mohd, H.B. Moon, H. Nakata, K. Kannan, Bisphenol S in urine from the United States and seven Asian countries: occurrence and human exposures, *Environ. Sci. Technol.* 46 (2012) 6860–6866.
 - [16] X. Sun, J. Wang, Y. Li, J. Jin, B. Zhang, S.M. Shah, X. Wang, J. Chen, Highly selective dummy molecularly imprinted polymer as a solid-phase extraction sorbent for five bisphenols in tap and river water, *J. Chromatogr. A* 1343 (2014) 33–41.
 - [17] H. Ullah, S. Jahan, Q.U. Ain, G. Shaheen, N. Ahsan, Effect of bisphenol S exposure on male reproductive system of rats: a histological and biochemical study, *Chemosphere* 152 (2016) 383–391.
 - [18] S. Eladak, T. Grisin, D. Moisson, M.J. Guerquin, T. N'Tumba-Byn, S. Pozzi-Gaudin, A. Benachi, G. Livera, V. Rouiller-Fabre, R. Habert, A new chapter in the bisphenol A story: bisphenol S and bisphenol F are not safe alternatives to this compound, *Fertil. Steril.* 103 (2015) 11–21.
 - [19] M. Ike, M.Y. Chen, E. Danzl, K. Sei, M. Fujita, Biodegradation of a variety of bisphenols under aerobic and anaerobic conditions, *Water Sci. Technol.* 53 (2006) 153–159.
 - [20] Y. Liu, X. He, Y. Fu, D.D. Dionysiou, Degradation kinetics and mechanism of oxytetracycline by hydroxyl radical-based advanced oxidation processes, *Chem. Eng. J.* 284 (2016) 1317–1327.
 - [21] J.A. Khan, X. He, N.S. Shah, H.M. Khan, E. Hapeshi, D. Fatta-Kassinos, D.D. Dionysiou, Kinetic and mechanism investigation on the photochemical degradation of atrazine with activated H₂O₂, S₂O₈²⁻ and HSO₅⁻, *Chem. Eng. J.* 252 (2014) 393–403.
 - [22] N.S. Shah, X. He, H.M. Khan, J.A. Khan, K.E. O'Shea, D.L. Boccelli, D.D. Dionysiou, Efficient removal of endosulfan from aqueous solution by UV-C/peroxides: a comparative study, *J. Hazard. Mater.* 263 (Pt 2) (2013) 584–592.
 - [23] M. Klavarioti, D. Mantzavinos, D. Kassinos, Removal of residual pharmaceuticals from aqueous systems by advanced oxidation processes, *Environ. Int.* 35 (2009) 402–417.
 - [24] A. Tsitonaki, B. Petri, M. Crimi, H. Mosbæk, R.L. Siegrist, P.L. Bjerg, In situ chemical oxidation of contaminated soil and groundwater using persulfate: a review, *Crit. Rev. Environ. Sci. Technol.* 40 (2010) 55–91.
 - [25] M.G. Antoniou, A.A. de la Cruz, D.D. Dionysiou, Degradation of microcystin-LR using sulfate radicals generated through photolysis, thermolysis and e-transfer mechanisms, *Appl. Catal. B: Environ.* 96 (2010) 290–298.
 - [26] C.J. Liang, H.W. Su, Identification of sulfate and hydroxyl radicals in thermally activated persulfate, *Ind. Eng. Chem. Res.* 48 (2009) 5558–5562.
 - [27] Y.H. Guan, J. Ma, X.C. Li, J.Y. Fang, L.W. Chen, Influence of pH on the formation of sulfate and hydroxyl radicals in the UV/peroxymonosulfate system, *Environ. Sci. Technol.* 45 (2011) 9308–9314.
 - [28] C. Luo, J. Jiang, J. Ma, S. Pang, Y. Liu, Y. Song, C. Guan, J. Li, Y. Jin, D. Wu, Oxidation of the odorous compound 2,4,6-trichloroanisole by UV activated persulfate: kinetics, products, and pathways, *Water Res.* 96 (2016) 12–21.
 - [29] A. Ghauch, A. Baalbaki, M. Amasha, R. El Asmar, O. Tantawi, Contribution of persulfate in UV-254 nm activated systems for complete degradation of chloramphenicol antibiotic in water, *Chem. Eng. J.* 317 (2017) 1012–1025.
 - [30] J. Zou, J. Ma, L. Chen, X. Li, Y. Guan, P. Xie, C. Pan, Rapid acceleration of ferrous iron/peroxymonosulfate oxidation of organic pollutants by promoting Fe(III)/Fe(II) cycle with hydroxylamine, *Environ. Sci. Technol.* 47 (2013) 11685–11691.
 - [31] C. Tan, N. Gao, W. Chu, C. Li, M.R. Templeton, Degradation of diuron by persulfate activated with ferrous ion, *Sep. Purif. Technol.* 95 (2012) 44–48.
 - [32] S. Naim, A. Ghauch, Ranitidine abatement in chemically activated persulfate systems: assessment of industrial iron waste for sustainable applications, *Chem. Eng. J.* 288 (2016) 276–288.
 - [33] G. Ayoub, A. Ghauch, Assessment of bimetallic and trimetallic iron-based systems for persulfate activation: application to sulfamethoxazole degradation, *Chem. Eng. J.* 256 (2014) 280–292.
 - [34] A. Ghauch, G. Ayoub, S. Naim, Degradation of sulfamethoxazole by persulfate assisted micrometric FeO in aqueous solution, *Chem. Eng. J.* 228 (2013) 1168–1181.
 - [35] W.S. Chen, Y.C. Su, Removal of dinitrotoluenes in wastewater by sono-activated persulfate, *Ultrason. Sonochem.* 19 (2012) 921–927.
 - [36] B. Li, L. Li, K. Lin, W. Zhang, S. Lu, Q. Luo, Removal of 1,1,1-trichloroethane from aqueous solution by a sono-activated persulfate process, *Ultrason. Sonochem.* 20 (2013) 855–863.
 - [37] O.S. Furman, A.L. Teel, R.J. Watts, Mechanism of base activation of persulfate, *Environ. Sci. Technol.* 44 (2010) 6423–6428.
 - [38] S. Yang, X. Yang, X. Shao, R. Niu, L. Wang, Activated carbon catalyzed persulfate oxidation of Azo dye acid orange 7 at ambient temperature, *J. Hazard. Mater.* 186 (2011) 659–666.
 - [39] G. Fang, J. Gao, D.D. Dionysiou, C. Liu, D. Zhou, Activation of persulfate by quinones: free radical reactions and implication for the degradation of PCBs, *Environ. Sci. Technol.* 47 (2013) 4605–4611.
 - [40] Y. Yang, J. Jiang, X. Lu, J. Ma, Y. Liu, Production of sulfate radical and hydroxyl radical by reaction of ozone with peroxymonosulfate: a novel advanced oxidation process, *Environ. Sci. Technol.* 49 (2015) 7330–7339.
 - [41] M. Zhang, X. Chen, H. Zhou, M. Murugananthan, Y. Zhang, Degradation of p-nitrophenol by heat and metal ions co-activated persulfate, *Chem. Eng. J.* 264 (2015) 39–47.
 - [42] C. Tan, N. Gao, Y. Deng, N. An, J. Deng, Heat-activated persulfate oxidation of diuron in water, *Chem. Eng. J.* 203 (2012) 294–300.
 - [43] Y. Ji, C. Dong, D. Kong, J. Lu, Q. Zhou, Heat-activated persulfate oxidation of atrazine: implications for remediation of groundwater contaminated by herbicides, *Chem. Eng. J.* 263 (2015) 45–54.
 - [44] H. Guo, N. Gao, Y. Yang, Y. Zhang, Kinetics and transformation pathways on oxidation of fluoroquinolones with thermally activated persulfate, *Chem. Eng. J.* 292 (2016) 82–91.
 - [45] A. Ghauch, A.M. Tuqan, Oxidation of bisoprolol in heated persulfate/H₂O systems: kinetics and products, *Chem. Eng. J.* 183 (2012) 162–171.
 - [46] C.J. Liang, C.J. Bruell, M.C. Marley, K.L. Sperry, Thermally activated persulfate oxidation of trichloroethylene (TCE) and 1,1,1-trichloroethane (TCA) in aqueous systems and soil slurries, *Soil Sediment Contam.* 12 (2003) 207–228.
 - [47] K.C. Huang, Z. Zhao, G.E. Hoag, A. Dahmani, P.A. Block, Degradation of volatile organic compounds with thermally activated persulfate oxidation, *Chemosphere* 61 (2005) 551–560.
 - [48] C. Liang, C.F. Huang, N. Mohanty, R.M. Kurakalva, A rapid spectrophotometric determination of persulfate anion in ISCO, *Chemosphere* 73 (2008) 1540–1543.
 - [49] P. Maruthamuthu, P. Neta, Phosphate radicals. Spectra, acid-base equilibria, and reactions with inorganic compounds, *J. Phys. Chem.* 82 (1978) 710–713.
 - [50] C. Liang, C.J. Bruell, Thermally activated persulfate oxidation of trichloroethylene: experimental investigation of reaction orders, *Ind. Eng. Chem. Res.* 47 (2008) 2912–2918.
 - [51] A. Ghauch, A.M. Tuqan, N. Kibbi, Ibuprofen removal by heated persulfate in aqueous solution: a kinetics study, *Chem. Eng. J.* 197 (2012) 483–492.
 - [52] Y. Fan, Y. Ji, D. Kong, J. Lu, Q. Zhou, Kinetic and mechanistic investigations of the degradation of sulfamethazine in heat-activated persulfate oxidation process, *J. Hazard. Mater.* 300 (2015) 39–47.
 - [53] M. Nie, Y. Yang, Z. Zhang, C. Yan, X. Wang, H. Li, W. Dong, Degradation of chloramphenicol by thermally activated persulfate in aqueous solution, *Chem. Eng. J.* 246 (2014) 373–382.
 - [54] C. Liang, Z.S. Wang, N. Mohanty, Influences of carbonate and chloride ions on persulfate oxidation of trichloroethylene at 20 degrees C, *Sci. Total Environ.* 370 (2006) 271–277.
 - [55] G.V. Buxton, M. Bydder, G.A. Salmon, The reactivity of chlorine atoms in aqueous solution. Part II. The equilibrium $\text{SO}_4^{\cdot-} + \text{Cl}^- \rightleftharpoons \text{Cl}^\cdot + \text{SO}_4^{2-}$, *Phys. Chem. Chem. Phys.* 1 (1999) 269–273.
 - [56] C. Tan, N. Gao, Y. Deng, W. Rong, S. Zhou, N. Lu, Degradation of antipyrine by heat activated persulfate, *Sep. Purif. Technol.* 109 (2013) 122–128.
 - [57] C. Liang, Z.-S. Wang, C.J. Bruell, Influence of pH on persulfate oxidation of TCE at ambient temperatures, *Chemosphere* 66 (2007) 106–113.
 - [58] H.S. Fogler, *Elements of Chemical Reaction Engineering*, NJ, Englewood Cliffs, 1998.